

Photoacoustic molecular imaging with antibody-functionalized single-walled carbon nanotubes for early diagnosis of tumor

Liangzhong Xiang*

Yi Yuan*

Da Xing

Zhongmin Ou

Sihua Yang

Feifan Zhou

South China Normal University

Ministry of Education

Key Laboratory of Laser Life Science and Institute of

Laser Life Science

Guangzhou 510631, China

Abstract. Single-walled carbon nanotubes (SWNT) in a poly(ethylene)glycol solution are a biocompatible transporters with strong optical absorption in the near-infrared region, in which the biological tissue is almost transparent with very low absorbance. Here, antibody-functionalized SWNTs for tumor early detection with photoacoustic molecular imaging *in vivo* are reported. To lay the groundwork for this goal and insure system stability, images were collected in tissue simulating phantoms to determine appropriate detectable concentrations of SWNTs. Preliminary *in vitro* and *in vivo* results showed that a high contrast and a high efficient targeting of integrin $\alpha_v\beta_3$ positive U87 human glioblastoma tumours in mice could be achieved. The nontoxicity of functionalized SWNTs has also been demonstrated in our experiment; this feature ensures that SWNTs can be used for clinical applications. This study suggests that photoacoustic molecular imaging with antibody-functionalized SWNTs has the potential to be an effective early tumor diagnosis method. © 2009 Society of Photo-Optical Instrumentation Engineers. [DOI: 10.1117/1.3078809]

Keywords: photoacoustic imaging; single-walled carbon nanotubes; molecular imaging; tumor targeting; $\alpha_v\beta_3$ positive.

Paper 08236SSRR received Jul. 15, 2008; revised manuscript received Nov. 13, 2008; accepted for publication Nov. 15, 2008; published online Mar. 4, 2009.

1 Introduction

Molecular imaging refers to remote-sensing the characteristics of the biological process and interactions between molecules at the molecular level.¹ It has great potential for the early detection and more effective treatment of diseases, because aberrations at the cellular and molecular levels occur much earlier than morphological changes. Molecular imaging methods have developed for many different imaging modalities, including optical imaging,² ultrasonic imaging,³ magnetic resonance imaging,⁴ and nuclear-medicine-based imaging.⁵ Here, we provide the photoacoustic (PA) imaging technique using molecularly targeted single-walled carbon nanotubes (SWNTs) to detect highly proliferative cancerous cells.

PA imaging is a new imaging modality under preclinical development that has been applied to several biomedical applications for obtaining structural and functional information, including diagnosing breast cancer,^{6,7} imaging of gene overexpression,⁸ monitoring of vascular damage during photodynamic therapy treatment of tumors,⁹ noninvasive monitoring of traumatic brain injury and post-traumatic rehabilitation,¹⁰ and imaging of cerebrovascular activities in small animals and hemoglobin oxygen saturation variations.¹¹

PA imaging using near-infrared (NIR) illumination in the range of 700–1000 nm has attracted the most attention, because light can penetrate several centimeters into tissue at these wavelengths. Ideally, the tissue medium should have low optical absorption for deep penetration, while the objects of interest (such as tumors in cancer detection) should have high absorption for the best image contrast. Exogenous staining can provide high contrast when the natural optical contrast is not sufficient. Several PA imaging studies utilized various NIR absorbing agents, such as indocyanine green,¹² and several types of gold nanoparticles, such as nanoshells¹³ and nanorods.¹⁴

SWNTs are an important class of artificial nanomaterials with remarkable mechanical, thermal, electronic, and optical properties. These properties suggest diverse future biomedical uses in areas such as targeted chemotherapeutics, *in vitro* cell markers, diagnostic imaging contrast agents, biochemical sensors, and photoablative therapy agents. The high optical absorbance of SWNTs in the NIR regime causes heating under laser irradiation, which is useful for destroying cancer cells that are selectively internalized with nanotubes. Various groups have found that well-water-solubilized nanotubes with high hydrophilicity are nontoxic, even at high concentrations.¹⁵

We present here PA molecular imaging with antibody-functionalized SWNTs for tumor early detection *in vivo*. To lay the groundwork for this goal, optical properties of SWNTs

*Both authors contributed equally to this work.

Address all correspondence to: Da Xing, Ph.D., Professor, MOE Key Laboratory of Laser Life Science & Institute of Laser Life Science, South China Normal University, Guangzhou 510631, China. Tel: +86-20-8521-0089; Fax: +86-20-8521-6052; E-mail: xingda@scnu.edu.cn

for molecular imaging of cancer have been studied. Images were collected in tissue-simulating phantoms to determine appropriate detectable concentrations of SWNTs. Preliminary *in vitro* and *in vivo* results showed that a high contrast and a high efficient targeting of integrin $\alpha_v\beta_3$ positive U87 human glioblastoma tumors in mice could be achieved. The nontoxicity of functionalized SWNTs has also been demonstrated in our experiment.

2 Materials and Methods

2.1 Materials

In our experiments, SWNTs were purchased from the Chinese Academy of Sciences (Chengdu, China). Nude mice were purchased from Sun Yat-Sen University (Guangzhou, China). Phospholipid-Poly(ethylene)glycol₂₀₀₀ (PL-PEG) was purchased from Avanti Polar Lipids, Inc. (Shanghai, China). Integrin $\alpha_v\beta_3$ antibody was purchased from Santa Cruz Biotechnology Inc. (Santa Cruz, California, USA), and Protein A was purchased from Bei Jing Biosynthesis Biotechnology Co., Ltd. (Beijing, China).

2.2 Administration of SWNTs

SWNTs were sonicated in an aqueous solution of PL-PEG at a ratio of 1 mg SWNTs: 1 mg PL-PEG: 1 mL water for 6 h, followed by centrifugation at 1000 g for 1 h. Then, the supernatant was collected and underwent an additional centrifugation at 24,000 g for 6 h to obtain well-suspended PL-PEG-functionalized SWNTs in the supernatant. Excess phospholipids were thoroughly removed by repeated filtration through 100 kDa filters (Millipore) and rinsed thoroughly with water, then resuspended SWNTs in either water or phosphate-buffered saline (PBS) by sonication for 1 h. The PL-PEG-functionalized SWNTs (denoted as SWNT-PEG-COOH) were finally resuspended in PBS.

2.3 Anti-integrin $\alpha_v\beta_3$ Conjugation to SWNTs

SWNT-PEG-COOH solution was reacted with *N*-hydroxysulphosuccinimide (NHS) in the presence of 1-ethyl-3-[3-(dimethylamino)-propyl] carbodiimide at 1:1:1 molar ratio, then Protein A was mixed with the SWNT-PEG-COOH solution at pH 7.4 and incubated for 4 h. The SWNT-PEG-Protein A was filtrated through 100 KDa filters (Millipore) to remove excess Protein A. Then, integrin $\alpha_v\beta_3$ antibody was added into a solution of SWNT-PEG-Protein A. The mixture was allowed to react for 4 h at room temperature and protected from light. After reaction, the solution was dialyzed against PBS using a membrane (molecular weight cutoff=500 KDa) to remove dissociative anti-integrin $\alpha_v\beta_3$. The dialysis was carried out for 3 days with frequent replacement of the buffer to obtain the final sample SWNT-PEG-Anti-integrin $\alpha_v\beta_3$ solution (see Fig. 1).

2.4 Cell Lines and the Animal Model

U87MG human glioblastoma cancer cell lines (from American Type Culture Collection) were cultured under standard conditions. The U87MG tumor models were generated by subcutaneous injection of 5×10^6 cells in 50 μ L PBS into the back of the nude balb/c mice. PEGylated SWNTs were intramuscular-injected into the tumor-free nude mice tail for

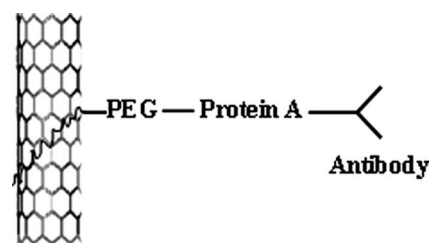


Fig. 1 Water-soluble SWNT functionalized with PEG and integrin $\alpha_v\beta_3$ antibodies. Schematic drawings of noncovalently functionalized SWNT-PEG₂₀₀₀ with Protein A and integrin $\alpha_v\beta_3$ antibody. The hydrophobic carbon chains of the phospholipids strongly bind to the side-walls of the SWNTs, and the PEG chains render water solubility to the SWNTs. The integrin $\alpha_v\beta_3$ antibody on the SWNTs are used to specifically target the integrin $\alpha_v\beta_3$ -positive tumor.

the *in vivo* PA molecular imaging experiment. Targeted SWNTs with anti-integrin $\alpha_v\beta_3$ molecules were intravenously injected into the tumor-bearing nude mice tail veins for tumor-targeting experiment

2.5 PA Molecular Imaging System for In Vivo SWNTs Selective Targeting

The PA molecular imaging system for *in vivo* SWNTs selective targeting is shown in Fig. 2. The photoacoustic signal is captured by a linear ultrasound transducer array (L7L38A, SIUI). The 128 elements piezoelectric linear transducer has a 7.5-MHz central frequency and a 70% nominal bandwidth. The physical dimensions of the elements are given by an elemental elevation aperture of 10 mm and a lateral pitch of 300 μ m. Each element of the transducer array has a thin cylinder ultrasonic lens that produces a geometric focus approximately 35 mm in front of the transducer array to select the 2-D image plane and suppress the out-of-plane signals.

A frequency-doubled Nd:yttrium aluminum garnet laser pumping an optical parametric oscillator (Vibrant 532 I, Oportek, Carlsbad, CA) was employed to provide 690–960 nm laser light with a pulse duration of 10 ns and a pulse repetition rate of 10 Hz. The laser beam was expanded and homogenized to provide an incident energy density of <10 mJ/cm² and a beam diameter of 1 cm to irradiate the sample for generating photoacoustic signals. A 25 MHz clock signal, provided by a control circuit, was divided into 10 Hz for triggering the pulse laser and controlling the multielement linear transducer array to acquire photoacoustic signals. The signals from the transducers, after preprocessing, including ultralow-noise time-gain compensate amplifiers, anti-aliasing bandpass filters, analog-to-digital converters, and several beamforming strategies (various f-number, aperture apodization, element size, etc.), were acquired with the NI PCI-6541 High-Speed Digital Wfm (50 MHz, selectable; voltage, 32 channels, 1 Mbit/channel). The collected data were stored in a computer for later processing. Next, the multielement linear transducer array was driven by a step motor to circularly scan around the sample, detecting the photoacoustic signals in the imaging plane at each position. The linear transducer array and the samples were both immersed in a tank of water for better coupling. The induced photoacoustic waves were captured every 18 deg., and a total of 20 positions of photoacoustic waves are recorded for a full view of the circularly scan-

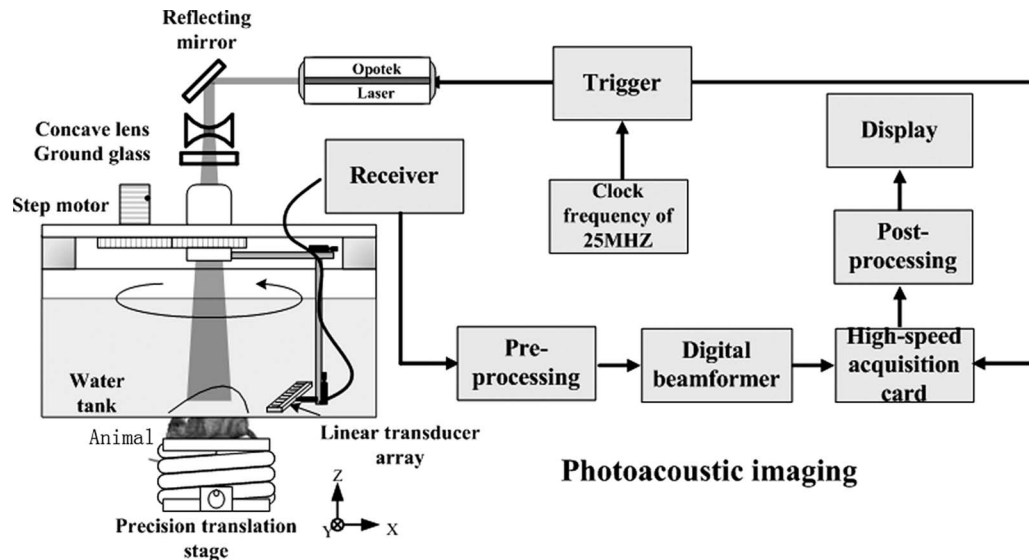


Fig. 2 Schematic of the experimental setup for the photoacoustic molecular imaging system. For optical absorption distribution reconstruction, the photoacoustic signal is captured by a linear ultrasound transducer array (L7L38A, SIUI). The 128 elements piezoelectric linear transducer has a 7.5-MHz central frequency and a 70% nominal bandwidth. An OPO-provided 750-nm laser beam is expanded and homogenized by the concave lens and the ground glass to irradiate on the backs of the mice. The linear ultrasound transducer array, driven by a computer-controlled step motor to scan around the mice, captures the PA signal after targeted SWNTs injection.

ning angle. After the 128×20 series data were transferred to the computer, further postprocessing was done using the MATLAB program (version 7.0, Mathworks). Projections were calculated with the improved limited-field filtered back projection algorithm.¹⁶ At last, the photoacoustic images were shown on the display.

3 Results

3.1 Optical Properties of SWNTs for PA Molecular Imaging

SWNTs were dispersed in the aqueous phase by noncovalently adsorbing PL-PEGs. Figure 3 presents visible spec-

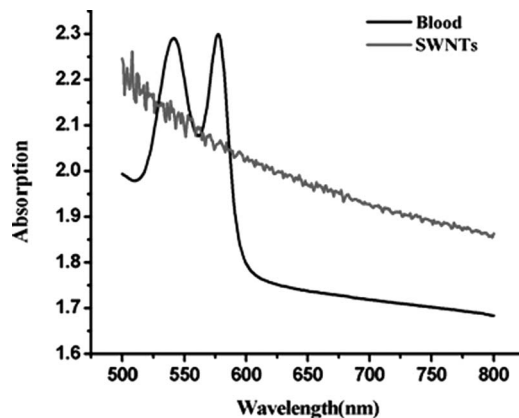


Fig. 3 VIS/NIR absorption spectra of the initial blood and functionalized SWNT samples in water. Absorption spectra of functionalized SWNTs were compared with pure blood absorption at the same concentration. The two absorption spectra are significantly different and clearly show that the SWNT can enhance absorption in the NIR region, where the optical transmission through biological tissues is optimal.

trometry (VIS)/NIR absorption spectra of the initial blood and functionalized SWNT samples in water. Absorption spectra of functionalized SWNTs were compared with pure blood absorption at the same concentration. The two absorption spectra are significantly different and clearly show that the SWNT can enhance absorption in the NIR region, in which the biological tissue is almost transparent with very low absorbance. Longer wavelengths are more desirable, as the depth of penetration through the tissues is increased; the photoacoustic spectra suggest that 750 nm is the preferable wavelength, because the photoacoustic signal of the SWNTs is higher than blood absorption at that wavelength. The high absorbance of SWNTs in the NIR originates from electronic transitions between the first or second van Hove singularities of the nanotubes.¹⁷ High optical absorbance of SWNTs in the 700–1100-nm NIR window transparent to biological systems is exploited in the current work at a single wavelength by using a 750-nm pulse laser for radiation.

In contrast to NIR-absorbing dyes, the absorption properties of SWNTs are dependent upon a rigid structure rather than on molecular orbital electronic transitions. SWNTs are also not susceptible to photobleaching, a problem commonly associated with other absorbing dyes. These features make SWNTs suitable as a contrast agent for photoacoustic molecular imaging in the NIR region.

3.2 SWNTs for Photoacoustic Molecular Imaging

This experiment was performed to determine the concentration of SWNTs as a NIR contrast agent for effective enhancement in photoacoustic molecular imaging. The optical absorption spectrum of PL-PEG functionalized SWNT was tested at different concentrations [see Fig. 4(a)]. Linear curve fitting for peak absorption at a wavelength of 750 nm was shown in Fig. 4(b). For the PA signal peak intensity of different concentrations of SWNT solution, linear curve fitting for 750 nm

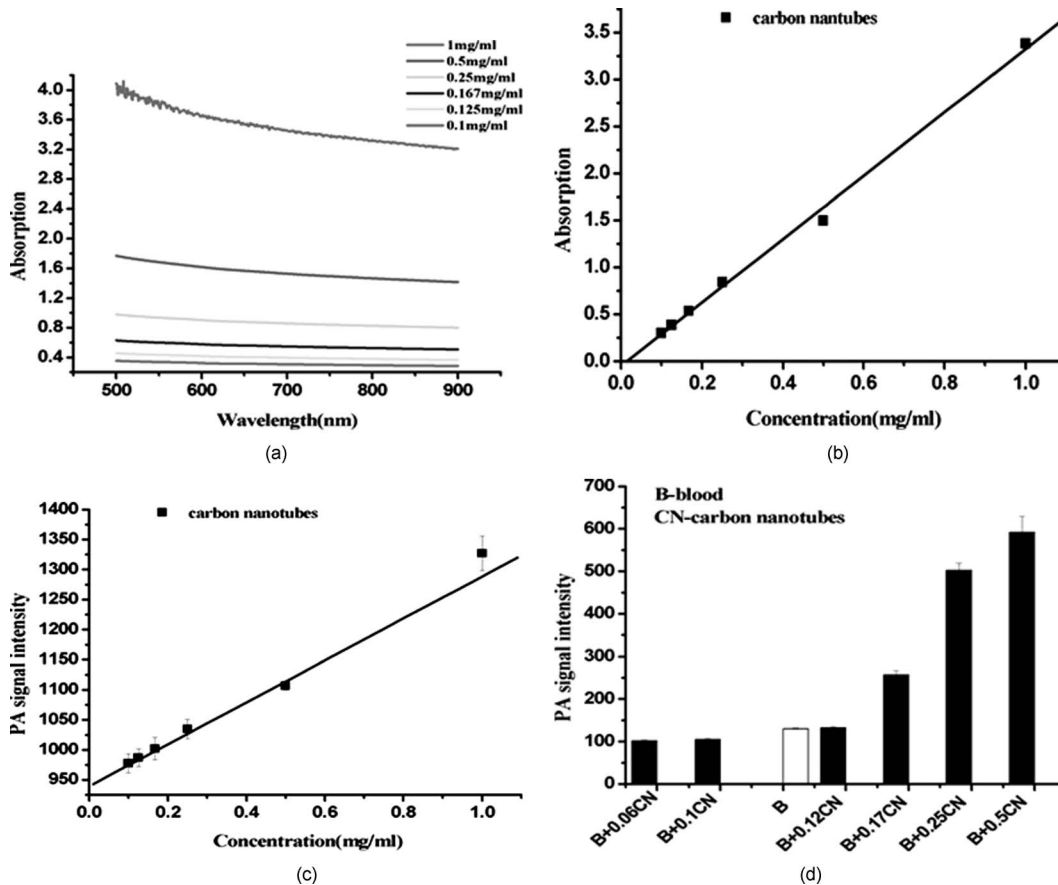


Fig. 4 SWNTs as IR contrast agent with varying concentrations for photoacoustic molecular imaging. (a) Absorption spectra of PEG₂₀₀₀-functionalized SWNT suspensions in PBS with varying concentrations. (b) Linear fitting of peak absorbance of spectrum versus concentration of SWNTs at 750 nm. (c) PA signal peak intensity of different concentrations of SWNT solution; linear curve fitting for absorption of 750 nm was evaluated to estimate the concentration of SWNTs. (d) Different concentrations of SWNT solution suspended in blood *in vitro*. The series of experiments indicated that a SWNT solution concentration of 0.17 mg/mL can achieve effective enhancement.

absorption was evaluated to estimate the concentration of SWNTs [see Fig. 4(c)]. Different concentrations of SWNT solution mixed with blood were also investigated *in vitro* to estimate the appropriate concentration for *in vivo* application in Fig. 4(d).

These data suggest that a SWNT solution concentration of 0.17 mg/mL can achieve effective enhancement using a 750 nm pulse laser. We thus expect, based on the concentrations of SWNTs expected to be bound *in vivo*, that it will be possible to detect the uptake of the proposed *in vivo* tumor probe.

3.3 *In Vitro* PA Measurements

SWNTs as IR contrast agent for photoacoustic molecular imaging were demonstrated in an *in vitro* experiment. Two identical 0.8-mm-diameter tubes, one with 300 μ L SWNTs of 0.17 mg/mL and one with pure blood, were placed side by side in the imaging tank at a depth of 10 mm in a mimic phantom of Intralipid-20% dilution. The image in Fig. 5(a) was obtained by photoacoustic scanning by the linear transducer array and represents a clearer map of tube A containing SWNTs+blood than of tube B containing blood only. With the exogenous contrast agent, the optical absorption of the blood was increased, and the contrast between the vessels and

the background brain tissues was enhanced. Reconstructed profiles of these two tubes shown in Fig. 5(b) also show higher signal-to-noise ratios using a SWNT-enhanced sample than using blood only at the excitation wavelength of 750 nm.

3.4 Cellular Toxicity Tests of SWNTs

Cell cytotoxicity assay was performed with a colorimetric tetrazolium salt-based assay, Cell Counting Kit-8 (CCK8). To determine the cytotoxicity of SWNTs, tumor cells (1×10^3 per well) were cultured in a 96-well microplate for 24 h and then co-incubated with functionalized SWNTs of different concentrations for 12 h, rinsed with PBS, and incubated for another 72 h. OD450, with an absorbance value of 450 nm, was read with a 96-well plate reader (Infinite M200, Tecan, Switzerland) to determine the viability of the cells. The viability of cells was calculated as: cell viability (% of control) = $\text{OD}_{\text{Tre}} / \text{OD}_{\text{Con}} \times 100\%$ (where OD_{Tre} was the absorbance value at 450 nm of treated cells and OD_{Con} was the absorbance value at 450 nm of control cells). Cell-toxicity tests (see Fig. 6) show that SWNTs display satisfactory biosafety at the dosages expected for *in vivo* applications.

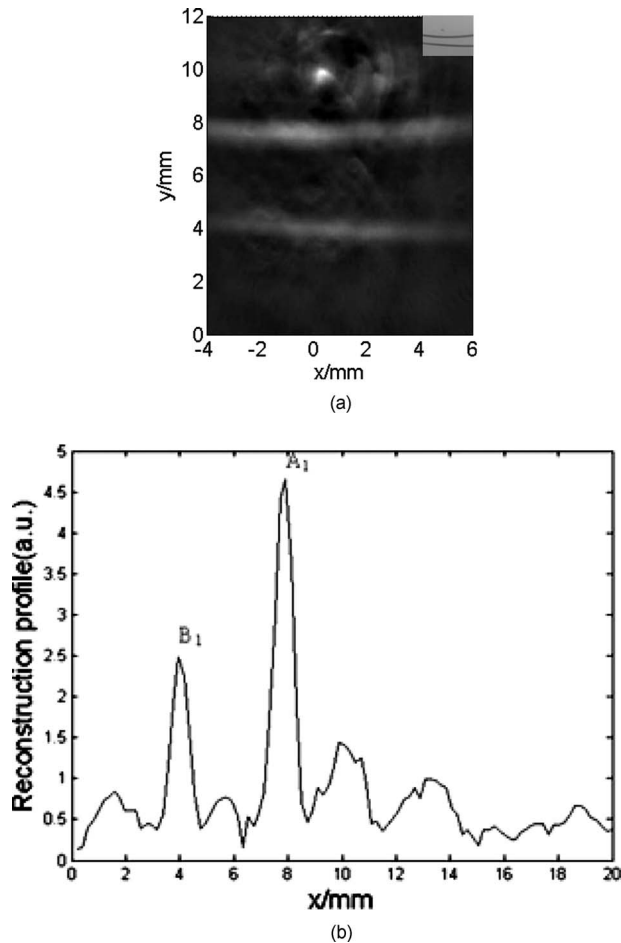


Fig. 5 SWNTs as IR contrast agent for photoacoustic imaging *in vitro*. (a) Photoacoustic images of A gel phantom with two tubes, tube A containing SWNTs+blood and tube B containing blood only. (b) The line normal to object axis profile of the reconstructed image shown in (a) with $x=0$ mm, which shows a better imaging contrast with enhanced SWNTs than blood only at a wavelength of 750 nm.

3.5 *In Vivo* PA Imaging of SWNTs

SWNTs as IR contrast agent for photoacoustic molecular imaging were demonstrated in an *in vivo* experiment. Female nude mice (20–25 g body weight) were employed in this work. General anesthesia was administered on the mice by an intramuscular injection of ketamine hydrochloride (44 mg/kg), xylazine hydrochloride (2.5 mg/kg), acepromazine maleate (0.75 mg/kg), and atropine (0.025 mg/kg). During the experiment, the mouse was placed on a water-circulating heating pad, and additional heating was provided by an overhead surgical lamp. During the data acquisition, the rat was provided pure oxygen for breathing, and the arterial blood oxygenation (SpO_2) level and heart rate were monitored by a pulse oximeter (8600 V, Nonin) with the fiberoptic probe wrapped around a paw of the animal. The SWNT was successively intramuscular-injected into the tail of the mouse at a dose of 300 μ L SWNTs dispersed in PBS with a concentration of 0.17 mg/mL. Image acquisition of the mouse tail began approximately 120 min following administration.

Two of the photoacoustic angiographs of the rat tail are presented in Fig. 7(a) and 7(c). Compared to the tail image

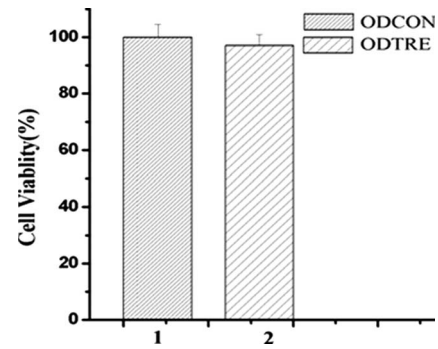


Fig. 6 Cell toxicity of SWNT measurement. The viability of cells was calculated as: cell viability (% of control)=ODTre/ODCon \times 100% (where ODTre was the absorbance value at 450 nm of treated cells and ODCon was the absorbance value at 450 nm of control cells). SWNT-treated cells show little decreased viability in the colorimetric tetrazolium salt-based assay at 4 days when compared to control cells (ODCon). With the CCK8 assay, at all concentrations, SWNT-treated cells also show no significantly decreased viability when compared to control cells.

based on the intrinsic optical contrast [Fig. 7(a)], the image with SWNTs contrast agent [Fig. 7(c)] shows greater clarity. It also shows a better signal-to-noise ratio when comparing Fig. 7(b) with 7(d).

3.6 *In Vivo* PA Imaging of SWNTs Targeted Tumor

In vivo PA imaging of SWNTs targeted tumor has been performed in this experiment. The targeted SWNTs with anti-integrin $\alpha_v\beta_3$ molecules and SWNTs-PEG (control group) were injected into the tail veins of two mice. In each mouse, the targeting process was imaged 2 h after injection.

Photoacoustic scanning was performed after tumor-cell inoculation for two weeks. The PA images of a U87 tumor for injections with targeted SWNTs and SWNTs-PEG (control group) in Fig. 8 demonstrate the specific targeting ability of the targeted SWNTs probe. The contrast is higher for the targeted SWNTs data postinjection (2 h after injection) within the tumor region [Fig. 8(b)] than for the SWNTs-PEG injection [Fig. 8(a)]. The contrast between the experimental group (targeted SWNTs injection) and the control group (SWNTs-PEG injection) indicated specific targeting of SWNTs targeted with anti- $\alpha_v\beta_3$ to U87 cells.

4 Discussion

Antibody-functionalized SWNTs have been designed for photoacoustic molecular imaging to specifically target early tumors. In the present study, preliminary *in vitro* and *in vivo* experiments were performed to lay the groundwork for this goal. The salient feature of this work is the use of functionalized SWNTs as both antibody shuttle and photoacoustic contrast agents. This can significantly suggest that photoacoustic molecular imaging with antibody-functionalized SWNTs has the potential to be an effective early tumor-diagnosis method.

Biocompatibility has been an important issue for *in vivo* applications of SWNTs. Results from analyses of SWNTs *in vivo* systemic toxicity tests (see Fig. 6) show that SWNTs are biocompatible and hemocompatible for *in vivo* tests. SWNTs exhibit satisfactory biosafety at the dosages expected for *in*

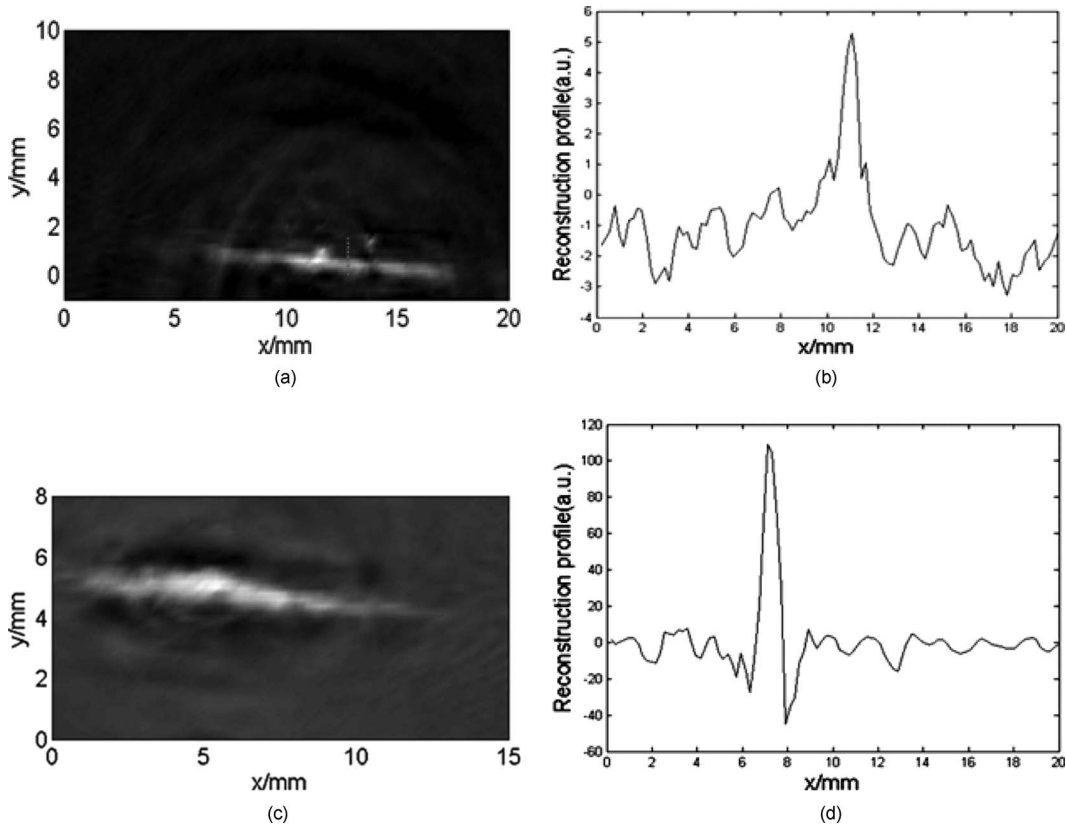


Fig. 7 *In vivo* PA imaging of SWNTs as contrast agent in mouse tail. (a) Control PA image without SWNTs-PEG₂₀₀₀ injection. (b) Reconstruction profile of mouse tail shown in (a). (c) PA image at 2 h after SWNTs-PEG injection. (d) Reconstruction profile of mouse tail shown in Fig. 7(d).

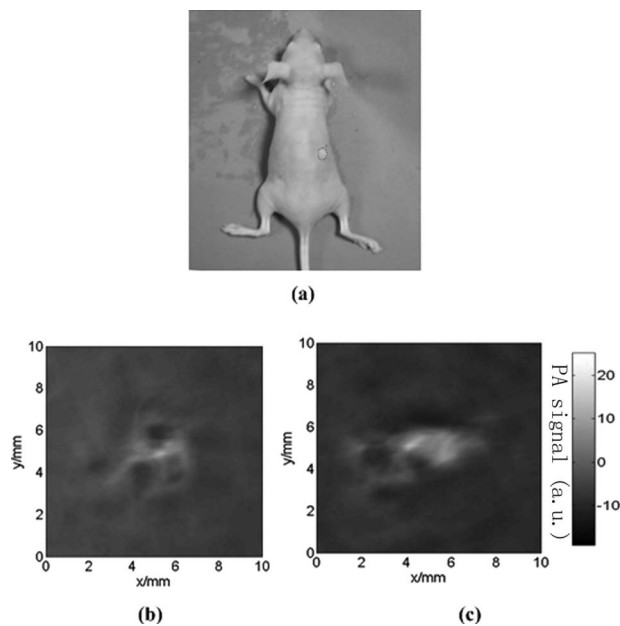


Fig. 8 *In vivo* PA imaging of U87 tumor before and after injection of targeted SWNTs. The PA signals were generated by pulsed laser at a wavelength of 750 nm. (a) Photograph of U87 tumor on the back of nude mice. Dotted line shows the tumor area. (b) PA image at 2 h after SWNTs-PEG injection. (c) PA image at 2 h after SWNT-PEG2000-Protein A-anti-integrin $\alpha_v\beta_3$ injection.

in vivo applications. The results of an *in vivo* toxicity test for SWNTs administered to nude mice via tail-vein injection were also satisfactory, with all mice surviving the 2-month observation period.

In addition, the temporal biodistribution of SWNTs in mice was analyzed to determine their metabolic clearance in some literatures.^{18,19} Intravenous administration of these functionalized SWNTs indicated that SWNTs are not retained in any of the reticuloendothelial system organs (liver or spleen). SWNTs are rapidly cleared from systemic blood circulation through the renal excretion route. The observed rapid blood clearance and half-life (3 h) of f-SWNT has major implications for all potential clinical uses of carbon nanotubes.¹⁹ So, the PA signal began to obtain 2 h after SWNT injection.

The U87 glioblastoma tumor, which highly expresses integrin $\alpha_v\beta_3$, was clearly imaged by photoacoustic molecular imaging as shown in Fig. 8(b). Clinical translation of SWNT-PEG2000-ProteinA-anti- $\alpha_v\beta_3$ is critical for the maximum benefit of Abegrin-based anticancer agents, as imaging can provide a straightforward and convenient way to monitor the biological changes at the molecular level *in vivo*. Future developments of anti- $\alpha_v\beta_3$ -directed therapy and translation of these encouraging experimental data to clinical studies would be greatly facilitated by noninvasive techniques that allow serial studies of $\alpha_v\beta_3$ -positive tumors.

This work demonstrates that photoacoustic molecular imaging with antibody-functionalized SWNTs can be applied in early tumor detection. PA molecular imaging with targeted

SWNTs has been demonstrated using SWNTs on a U87 tumor model *in vivo*. The results reveal that information about the oncogene surface molecules of cancer cells can be obtained with PA techniques, which will help improve our understanding of cancer cells and develop effective diagnosis tools as well as indications for effective treatments. Safe and effective SWNT-based cancer diagnoses have great potential in the pharmaceutical industry and could also make significant contributions in the biomedical field.

Acknowledgments

This research is supported by the National Natural Science Foundation of China (Grants No. 30870676, No. 30627003, No. 30800261) and the Natural Science Foundation of Guangdong Province (Grant No. 7117865). We also acknowledge the technical assistance by Dr. Baoyan Wu and helpful conversations with Dr. Lei Huang.

References

1. K. Shah, A. Jacobs, X. O. Breakefield, and R. Weissleder, "Molecular imaging of gene therapy for cancer," *Gene Ther.* **11**, 1175–1187 (2004).
2. X. Gao, Y. Cui, R. M. Levenson, L. W. K. Chung, and S. Nie, "*In vivo* cancer targeting and imaging with semiconductor quantum dots," *Nat. Biotechnol.* **22**, 969–976 (2004).
3. D. B. Ellegala, H. Leong-Poi, J. E. Carpenter, A. L. Klibanov, S. Kaul, M. E. Shaffrey, J. Sklenar, and J. R. Lindner, "Imaging tumor angiogenesis with contrast ultrasound and microbubbles targeted to $\alpha_v\beta_3$," *Circulation* **108**, 336–341 (2003).
4. L. Josephson, M. F. Kircher, U. Mahmood, Y. Tang, and R. Weissleder, "Near-infrared fluorescent nanoparticles as combined MR/optical imaging probes," *Bioconjugate Chem.* **13**, 554–560 (2002).
5. S. R. Cherry, "*In vivo* molecular and genomic imaging: new challenges for imaging physics," *Phys. Med. Biol.* **49**, R13–R48 (2004).
6. A. A. Oraevsky, V. A. Andreev, A. A. Karabutov, R. D. Fleming, Z. Gatalica, H. Singh, and R. O. Esenaliev, "Laser optoacoustic imaging of breast: detection of cancer angiogenesis," *Proc. SPIE* **3597**, 352–363 (1999).
7. R. A. Kruger, K. D. Miller, H. E. Reynolds, W. L. Kiser, D. R. Reinecke, and G. A. Kruger, "Breast cancer *in vivo* contrast enhancement with thermoacoustic CT at 434 MHz-feasibility study," *Radiology* **216**, 279–283 (2000).
8. L. Li, R. Zemp, G. Lungu, G. Stoica, and L. V. Wang, "Photoacoustic imaging of lacZ gene expression *in vivo*," *J. Biomed. Opt.* **12**(02), 020504-1–3 (2007).
9. L. Zh. Xiang, D. Xing, H. M. Gu, D. W. Yang, S. H. Yang, L. M. Zeng, and W. R. Chen, "Real-time optoacoustic monitoring of vascular damage during photodynamic therapy treatment of tumor," *J. Biomed. Opt.* **12**, 014001-1–8 (2007).
10. S. H. Yang, D. Xing, Y. Q. Lao, D. W. Yang, L. M. Zeng, L. Zh. Xiang, and W. R. Chen, "Noninvasive monitoring of traumatic brain injury and post-traumatic rehabilitation with laser-induced photoacoustic imaging," *Appl. Phys. Lett.* **90**, 243902-1–3 (2007).
11. S. Yang, D. Xing, Q. Zhou, L. Zh. Xiang, and L. Q. Lao, "Functional imaging of cerebrovascular activities in small animals using high-resolution photoacoustic tomography," *Med. Phys.* **34**, 3294–3301 (2007).
12. K. M. Stantz, B. Liu, M. Cao, D. Reinecke, K. Miller, and R. Kruger, "Photoacoustic spectroscopic imaging of intra-tumor heterogeneity and molecular identification," *Proc. SPIE* **6086**, 608605 (2006).
13. Y. W. Wang, X. Y. Xie, X. D. Wang, G. Ku, K. L. Gill, D. P. O'Neal, G. Stoica, and L. H. V. Wang, "Photoacoustic tomography of a nanoshell contrast agent in the *in vivo* rat brain," *Nano Lett.* **4**(9), 1689–1692 (2004).
14. P. Ch. Li, W. W. Chen, C. K. Liao, C. D. Chen, K. C. Pao, C. R. C. Wang, Y. N. Wu, and D. B. Shieh, "Multiple targeting in photoacoustic imaging using bioconjugated gold nanorods," *Proc. SPIE* **6086**, 60860M (2006).
15. C. K. Paul, J. G. Christopher, K. L. Tonya, K. S. Howard, E. S. Richard, A. C. Steven, and R. B. Weisman, "Mammalian pharmacokinetics of carbon nanotubes using intrinsic near-infrared fluorescence," *Proc. Natl. Acad. Sci. U.S.A.* **103**(50), 18882–18886 (2006).
16. D. W. Yang, D. Xing, S. H. Yang, and L. Zh. Xiang, "Fast full-view photoacoustic imaging by combined scanning with a linear transducer array," *Opt. Express* **15**(23), 15566–15575 (2007).
17. M. B. Sergei, S. S. Michael, K. Carter, H. H. Robert, E. S. Richard, and R. B. Weisman, "Structure-assigned optical spectra of single-walled carbon nanotubes," *Science* **298**, 2361–2366 (2002).
18. Zh. Liu, W. B. Cai, L. N. He, N. Nakayama, K. Chen, X. M. Sun, X. Y. Chen, and H. J. Dai, "*In vivo* biodistribution and highly efficient tumour targeting of carbon nanotubes in mice," *Nat. Nanotechnol.* **2**(1), 47–52 (2007).
19. R. Singh, D. Pantarotto, L. Lacerda, G. Pastorin, C. Klumpp, M. Prato, A. Bianco, and K. Kostarelos, "Tissue biodistribution and blood clearance rates of intravenously administered carbon nanotube radiotracers," *Proc. Natl. Acad. Sci. U.S.A.* **103**(9), 3357–3362 (2006).